

Summary talk on Fiber Tower Calorimeter
for the Scintillation Calorimeter subgroups

CONF-890379--6
DE89 013005

Andrew P. White*, University of Florida

* Reporting for a collaboration involving:

University of Florida (J.K. Walker, A.P. White)

Florida State University (C. Johnson, H. Wahl)

Oak Ridge National Laboratory (T. Gabriel)

Introduction

We present here a new calorimeter design based on small scintillator tiles, lead absorber and wavelength shifting fiber readout. We have addressed all the major issues in SSC calorimetry and have developed a design with many advantageous features.

It has been well demonstrated²⁾ that the best resolution is obtained for a 'compensated' calorimeter. It is also well known how such compensation may be achieved by a suitable choice of active and passive materials and their relative thickness. One such choice is that of lead and scintillator for which the best thickness ratio is 4:1. This selection has been used in the development of the so-called spaghetti calorimeter (SPACAL) discussed at this workshop³⁾. The relative merits of this and many other designs (Liquid Argon, Warm Liquids, Silicon, ...) have been the subject of much discussion at SSC workshops⁴⁾ from which a number of critical issues have emerged for each design. In the present paper, we have addressed the issues raised in the SPACAL design and proposed an alternative, improved design. The SPACAL represents a significant step forward in calorimeter design, but there are always

MASTER
J/K

areas which can be improved in any design when it is subjected to detailed study. Specifically we have considered the areas of energy resolution, channeling, projective towers/calibration, longitudinal segmentation, and radiation sensitivity. We will now discuss each of these areas in turn.

Design Issues for SPACAL

1) Energy Resolution

For a lead-scintillator calorimeter the intrinsic hadronic energy resolution is limited (conservatively) to $\sigma/E \gtrsim 0.20/\sqrt{E}$ by fluctuations in nuclear binding energy loss effects. The SPACAL resolution is not yet at this limit. The resolution can be improved by increasing the sampling frequency. However, for SPACAL with 4 mm Pb: 1 mm scintillator there are already 25 fibers/cm². To increase the sampling frequency by a factor (say 2) in order to obtain a useful improvement in the sampling resolution (by $1/\sqrt{2}$) would lead to a factor of two increase in the number of fibers which is not a practical solution.

2) Channeling

For low angles of incidence of particles relative to the fiber axis there is a deterioration of the electromagnetic energy resolution. This is shown in Fig. 1 which, however, only gives the average size of this effect. A greater concern are the fluctuations about this average. Such effects can, for instance, lead to a high tail on the missing transverse energy distribution, thereby producing a troublesome background to many areas of new physics searches. The extent of this effect and its impact on specific physics processes needs a detailed Monte Carlo study, which to our knowledge has not yet been carried out.

3) Projective Geometry/Calibration

If one considers the implications for the SPACAL design of requiring a projective geometry, various options are possible: (a) Having all the fibers starting at the face of a block yet diverging in separation with increasing radius. This means a departure from the ideal 4:1 ratio for compensation; (b) Having some fibers starting at the face of a block, then adding fibers starting within the block to maintain the 4:1 ratio throughout. This means that some fibers will have ends that are not directly accessible for calibration purposes; and (c) Truncation of fibers in blocks with all fibers parallel in order to achieve the projective block profile. This means that the ends of all fibers are accessible, either at the front face or sides, when the block is not mounted in the calorimeter system, but some fiber ends are not accessible in the final configuration. Overall the choice is between a departure from the 4:1 ratio, and hence a variation of σ/E with depth, or loss of the ability to carry out a full calibration. [We note that there have been some alternative calibration schemes suggested, e.g., the use of radioactive sources on rods - the practical feasibility of such schemes remains to be demonstrated.]

4) Longitudinal Segmentation

In the present SPACAL design a significant distance is required (30 cm for a 2 m deep unit) to bring the fibers together for connection to the photo-sensitive readout device. In such a situation one would not try to longitudinally segment a SPACAL calorimeter system. However, there is a factor $O(10^3)$ rejection of hadrons against electrons obtainable from such a segmentation. A prudent calorimeter designer would not abandon this factor easily even though there is a strong correlation between longitudinal and transverse shower generation. [During the workshop the SPACAL group stated that an effective longitudinal segmentation is possible by a time analysis

of the calorimeter pulses. It is unclear how much of the 10^3 factor could be recovered in this manner and what the associated electronics cost would be.]

Fiber Tower Calorimeter Design

We will now describe the design of our calorimeter and how it addresses the issues raised above.

The basic idea is to use a combination of small scintillator plates and fiber readout. A schematic drawing of a FITCAL "tower" is shown in Fig. 2. The use of 0.5 mm scintillator with 2 mm of lead gives a factor of two increase in the sampling frequency over SPACAL. A factor of $\sqrt{2}$ improvement in the electromagnetic resolution is then expected as shown in Fig. 3. It is important to note that such an improvement has been measured and verified previously⁵⁾.

The light from the individual scintillator tiles is collected by a 1 mm fiber running the length of the tower and orthogonal to the tiles. A projective geometry is achieved by increasing the size of the tiles with radius.

The small size ($\approx 1 \times 1 \text{ cm}^2$ at the inner radius) of the tiles is of critical importance in the design. Previous calorimeters of the lead/scintillator sandwich variety have used plate sizes of 5 and 19 cm on a side. This has led to measured non-uniformities of response of 10% and 25%, respectively, when the location of incidence of a particle is scanned across a tile.

This is obviously unacceptable when one is aiming for a resolution with a stability of O(1%) as it is believed is required at the SSC. The critical parameter controlling the uniformity is $(r_0/L)^2$, where r_0 is the fiber radius and L is the length of the side of a scintillator tile. Our choice of $1 \times 1 \text{ cm}^2$ gives good uniformity and is well matched to the typical transverse dimension of an electromagnetic shower. We have carried out a test of uniformity of

response using a 1 mm fiber and a 1 x 1 cm² tile (thickness 800 μm as this was immediately available). The results indicate a non-uniformity at no more than the 1-2 %.

In practice a section of FITCAL module will be formed from a lead block with slots for the scintillator tiles (see Figure 4) and orthogonal holes for the fibers. The scintillator tiles will be injection molded which produces a high optical quality finish (millions of optical lenses have been produced using this technique). A small injection molding machine, for prototype tests, is being obtained by the University of Florida group. This will allow easy fabrication of tiles with various polymers and fluors. Advantages of the molding technique are the automatic forming of holes for the fibers, excellent mechanical reproducibility, low cost (we estimate less than 1 cent per tile) and rapid production (1 tile/ machine/sec).

The tiles will be inserted into plastic trays (see Figure 5) prior to insertion into the lead matrix. The trays, and covers, serve to optically isolate adjacent tiles, and facilitate insertion into the lead and location of the tiles for fiber threading. In addition the trays and covers will be made of reflecting plastic to boost the amount of the scintillation light collected by the fiber. The trays and covers will also be injection molded and we have satisfied ourselves that the necessary thin (100 μm) walls of the trays and covers can be reproduced with adherence to the required mechanical tolerances. The parts are also cheap (estimated cost ≈ 8 cents per 8 tile unit) and fast (1 unit per 4 sec.) to produce.

The wavelength shifting fiber will be 1 mm clad fiber with a fluor chosen to emit at $\lambda > 500$ nm, for extra protection against possible radiation

damage effects.

We propose to make the tiles and the wavelength shifting fiber out of siloxane materials being developed for these purposes at the University of Florida. Siloxane based scintillator has been shown to experience no loss of transmission or light output ($\lambda > 500 \text{ nm}$) for doses up to 10^7 Rad .

Summary of beneficial features of FITCAL

We now discuss those features of FITCAL where specific improvements are expected for our alternative design, beyond the improvement in energy resolution discussed above.

1) Reduced Channeling

In FITCAL one tile of approximate dimensions $1 \times 1 \text{ cm}^2$ is read out by a single fiber. This represents a factor of 25 reduction in the number of fibers relative to SPACAL. This factor is expected to result in a substantial reduction in the channeling effect as seen in Figure 1.

2) Projective Towers

The desired 4:1 Pb/Scintillator ratio is achieved throughout the depth of a FITCAL module by increasing the size of the tiles as the radius increases. In this way the 4:1 ratio is independent of the arrangement of the fiber readout with the beneficial effect of permitting fiber calibration. This should be contrasted with the SPACAL choice to maintain the 4:1 ratio in depth by constructing wedge shaped modules with all fibers parallel, but having, as a result, fibers truncated in depth where they cut the sloping edges of the wedge.

3) Calibration

Since all the fibers in FITCAL run the full depth of each module, or depth segment of a module, their ends are all accessible for calibration

purposes. This removes the need for complex schemes to access the buried ends of truncated fibers.

4) Longitudinal Segmentation

The large reduction in the number of fibers (factor 25 fewer) relative to the SPACAL allows the FITCAL fibers to be brought to the readout device in a much shorter distance than the 30 cm now required in SPACAL. This then reintroduces the possibility of a traditional longitudinal segmentation for FITCAL with accompanying benefits to electron/hadron separation without the need for a pre-shower counter in front of the calorimeter.

SSC implementation of FITCAL

We now consider how the FITCAL approach may be used in a calorimeter system for the SSC. We first define some of the basic parameters which emerged from our study groups as a starting point for the SSC detector design. The inner radius of the calorimeter was taken as 2m., which allows the possibility of a full tracking system inside the calorimeter. The extent of the central part of the calorimeter system along the beam direction was taken as approximately $\pm 4\text{m}$. A substantially larger central section can lead to problems of shower leakage for particles entering the calorimeter at low angles, while a shorter central section (eg. $\pm 2\text{m}$) enhances the problems of radiation damage and physical space near the beam axis for the lower angle sections of the end calorimeters. The calorimeter depth for containment was set at 10 interaction lengths. Finally, the calorimeter system was taken to extend down to $y=\pm 3$, being the maximum rapidity at which plastic scintillation calorimetry could have a 10 year lifetime when constructed using new scintillating material which is radiation hard up to a total dose of 10^7 Rads.

A r-z view of our SSC detector design is shown in Figure 6. The calorimeter is divided into three sections, one central and two end sections, to allow access to and insertion/withdrawal of the central tracking system. A crucial feature of the calorimeter system is that the individual modules are independently supported at their outer radius from an open massive support frame. This open frame, which is itself supported by the external muon steel, allows for the possibility of individual module servicing and replacement.

Figure 6 shows that an individual module would be divided into three longitudinal segments, one electromagnetic and two hadronic. We will now describe in detail how such a segmented module would be constructed and read out.

Each longitudinal segment consists of a wedge shaped lead matrix constructed as described earlier. A box section (See Fig. 7) provides the structural interconnection between the three lead blocks, and also contains the readout sections for the electromagnetic and first hadronic segments. An important feature of the box sections is that they are attached to the lead blocks within the profile of the latter. In this way there is no dead space or material generated between the modules. In order to further minimize the cracks and dead material we propose an innovative approach to signal readout from our modules. We shall optically encode the pulse heights of the sixteen channels (in our example) at the output of the multianode photomultiplier. The encoded signals will travel out of the module via a 0.1 mm optical quartz fiber operating at 10GHz. This optical fiber will exit via a channel contained within the profile of the module segments. There will be only three optical readout fiber bundles per module, one for each longitudinal segment. A further optical fiber connection will take the encoded signals from the outer radius of

the module to an optical decoder located at the Level 0 trigger electronics. (≈ 50 ft distance). Besides the advantage of minimal readout line space, this technique also offers faster readout than traditional cables and minimizes the number and cost of readout lines.

Low and high voltage power, and calibration fibers to exit the optical front plates of each segment, will also be fed through channels within the module profile. This approach of staying within the profile leads to a small number of lower density narrow holes through each module which, however, is clearly preferable to a gap between modules.

The calibration scheme for a module would be in two parts. First, since all fibers in a longitudinal section emerge from the front of that section, we would use an optical plate across the front of the section to allow illumination of all fibers from an input calibration light source fiber routed as described above. This tests all parts of the calorimeter system except the scintillator tiles. To test the tiles we use the second part of the calibration system consisting of glass fibers on some small number of towers coupled to the tiles. For these towers, the complete system would then be calibrated. The issue of tower size ($d(\eta).d(\phi)$) for our detector is connected with the broader question of whether or not to use a central magnetic field. Table 1 summarizes this choice for the case of a non-magnetic detector and a magnetic detector with the solenoid outside the calorimeter. The use of a magnetic field has consequences for the nature of the module readout via phototubes. There is, however, a program of research underway in connection with SPACAL to build a compact semiconductor diode device with high gain which would be much less sensitive to the presence of a magnetic field.

Electromagnetic Prototype

We have been approved and funded by the SSC Detector Development Office of the SSC Division of the DOE to initially construct an electromagnetic calorimeter prototype module. The transverse dimensions will be $8 \times 8 \text{ cm}^2$ giving 64 channels. Each channel/tower will have the composition shown in Figure 3. The overall appearance of the module plus readout is shown in Figures 8 and 9.

We are working on the development of techniques to fabricate the lead matrix, the scintillator tiles, and the scintillator trays. We view this work on production techniques, which could be extended to a much larger scale necessary for a full calorimeter system, as the most vital part of our prototype program, which will also include measurement in beam tests of the energy and position resolutions.

Following the construction and testing of the electromagnetic prototype, we are studying the requirements for the construction of a major prototype section of a full calorimeter system. This will include a full engineering analysis of full depth, multiple section modules, their incorporation into an overall calorimeter system, and all aspects of the optically encoded readout scheme described above.

DISCLAIMER

This report was prepared as an account of work sponsored by an agency of the United States Government. Neither the United States Government nor any agency thereof, nor any of their employees, makes any warranty, express or implied, or assumes any legal liability or responsibility for the accuracy, completeness, or usefulness of any information, apparatus, product, or process disclosed, or represents that its use would not infringe privately owned rights. Reference herein to any specific commercial product, process, or service by trade name, trademark, manufacturer, or otherwise does not necessarily constitute or imply its endorsement, recommendation, or favoring by the United States Government or any agency thereof. The views and opinions of authors expressed herein do not necessarily state or reflect those of the United States Government or any agency thereof.

Conclusions

We have presented a calorimeter design which has considerable potential, and satisfies all the requirements for an SSC calorimeter system. We have also shown how such a design can be incorporated into an SSC design. Prototype work is underway and we are working towards a proposal for the test construction of a major section of a calorimeter based on our technique.

References

- (1) M. Jacob, CERN - TH.5156/88.
- (2) R. Wigmans, Nucl. Instrum. Methods A259, 389 (1987).
- (3) R. DeSalvo, report on the spaghetti calorimeter at this workshop.
- (4) A.P. White, Calorimetry section of Non-Magnetic detector report from "Experiments, Detectors and Experimental Areas for the Supercollider," R. Donaldson and M.G.D. Gilchriese, eds., Berkeley, 1987, pp. 482-501.
- (5) B. Loehr, et al., DESY86-072, July 1986; H. Fessler, et al., MPI-PAE/Exp. E1.149, Feb. 1985.

TOWER SIZE ($\Delta y \Delta P$)

e.m.
hadronic

CHANNELS

e.m.
hadronic

COMMENTS

MAGNETIC

0.02 x 0.02
0.05 x 0.05

90,000
28,800

Coil outside CAL
→ Preserve Good
(σ/E)e.m.)^oind.

μ Momentum from Central
B field

1 section of μ i.d.
+ flux return

Electrons -P, E
→ coarser EM Towers

NON MAGNETIC

0.01 x 0.01
0.05 x 0.05

360,000
28,800

μ Momentum in
external system

Fine e.m.
segmentation for
electron ind.

NO PRE-SHOWER COUNTER

TABLE 1

ELECTROMAGNETIC ENERGY RESOLUTION

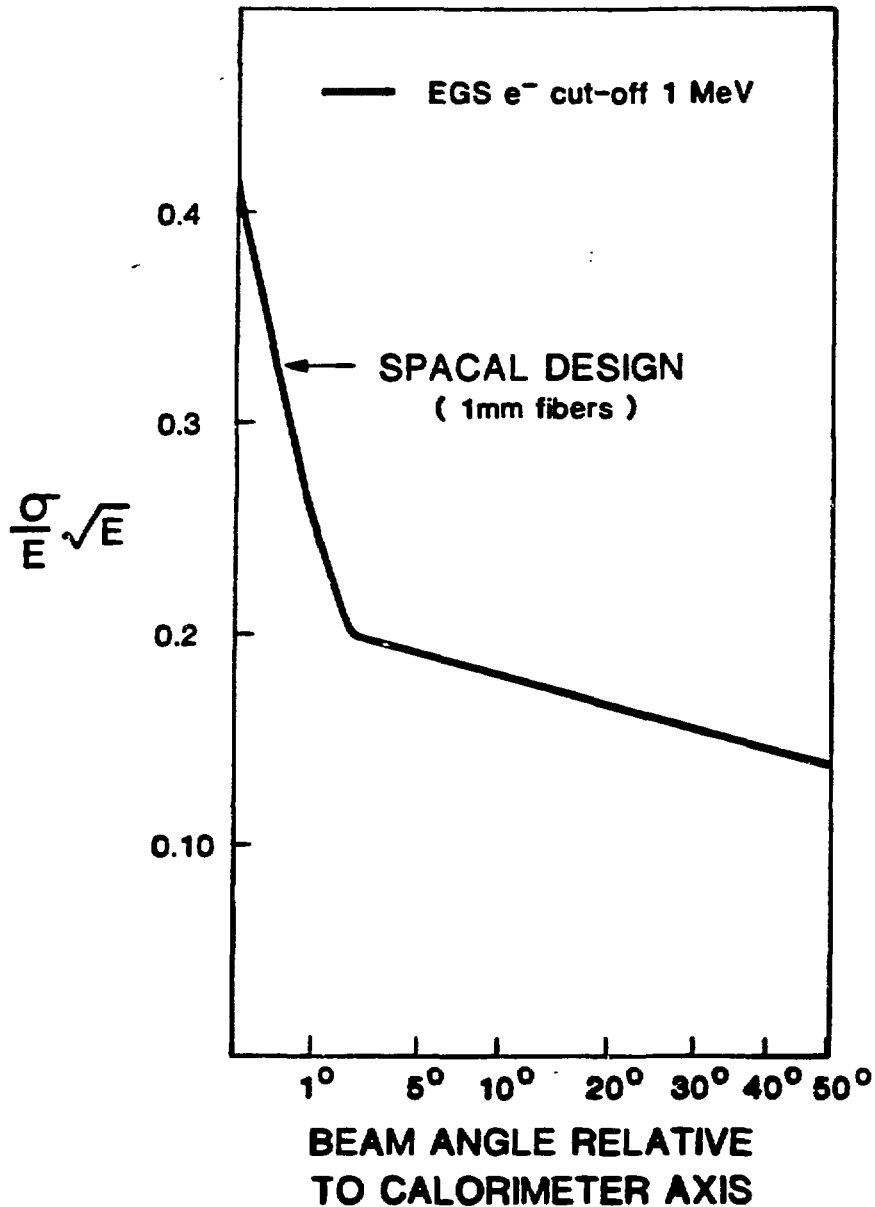


FIGURE 1 Deterioration of e.m. energy resolution at small angles of incidence. From the figure presented by O. Guildermeister of the SPACAL collaboration at the Fermilab $\bar{p}p$ Workshop June 20-23, 1988.

FITCAL - DETAILED STRUCTURE

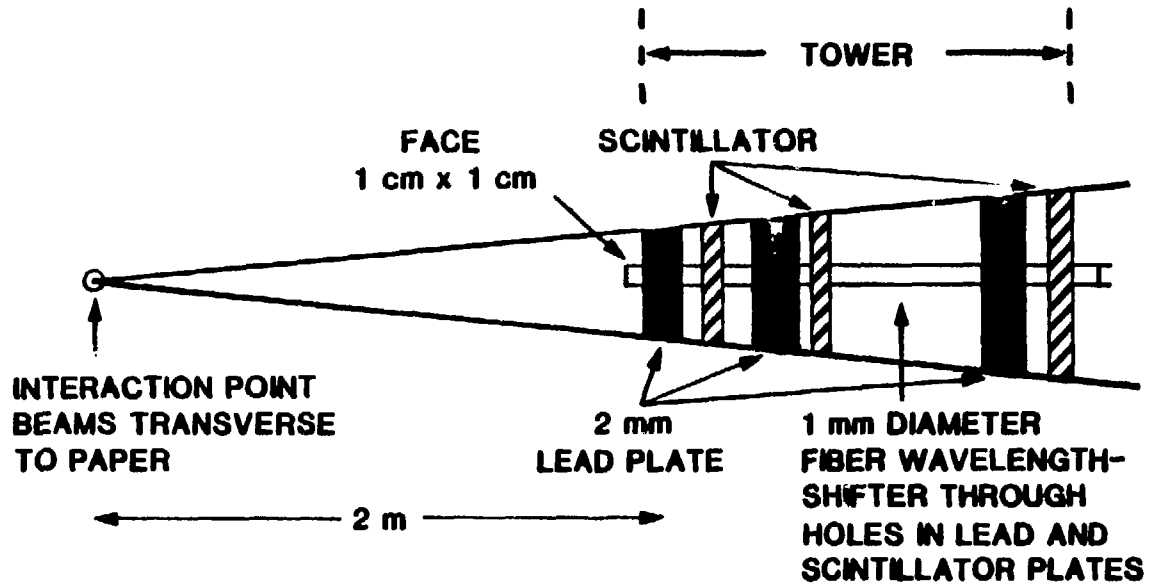


FIGURE 2 Conceptual drawing of a FITCAL tower.

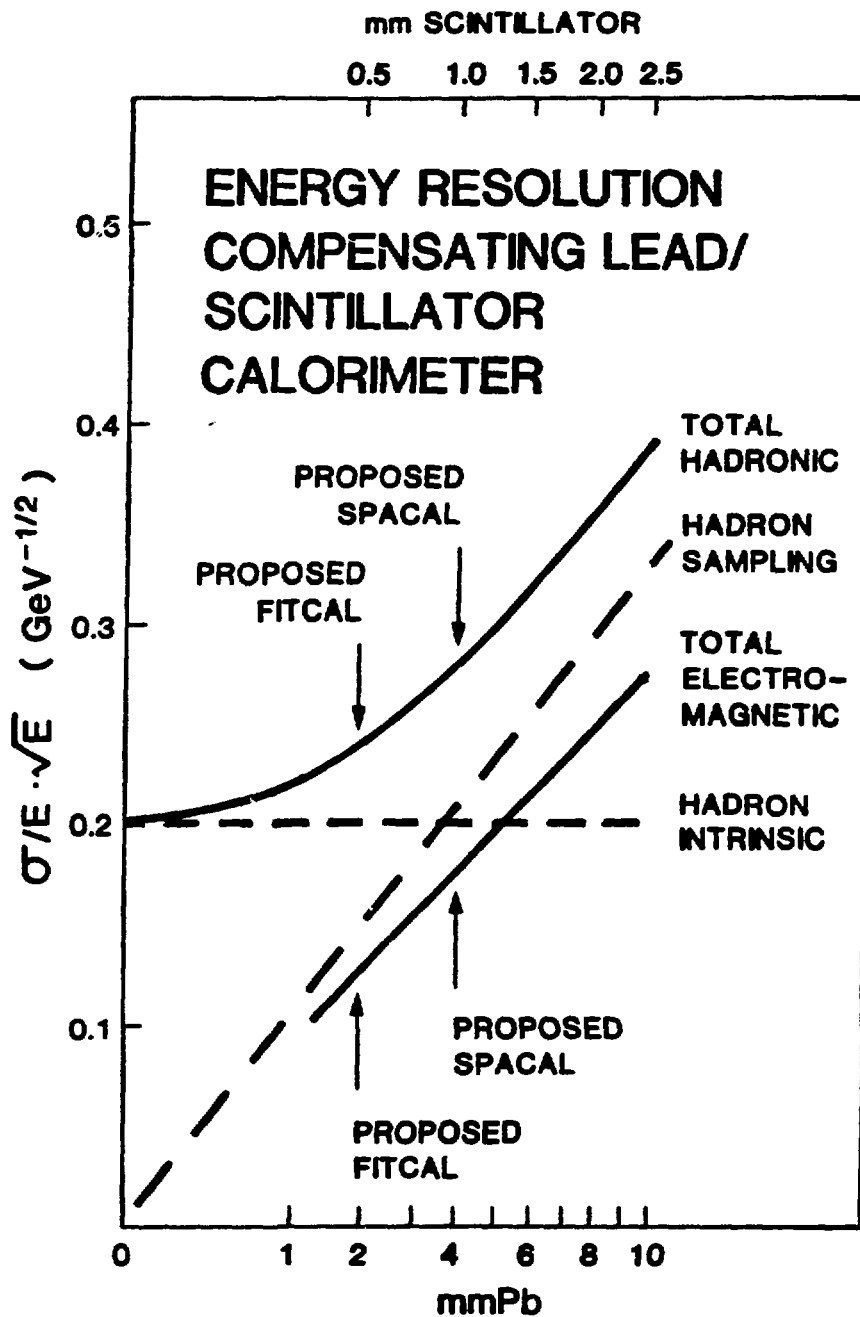
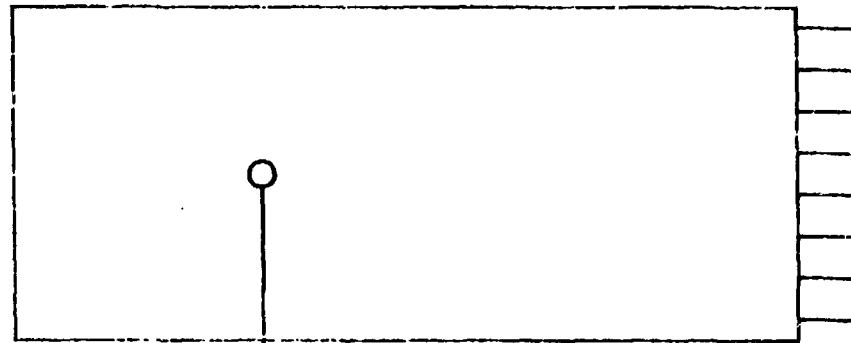
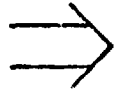


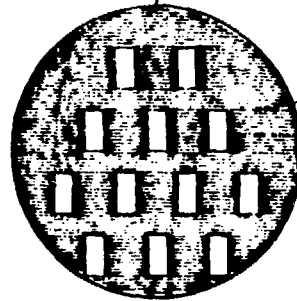
FIGURE 3 Lead/scintillator calorimeter energy resolutions as a function of lead thickness, keeping 4:1 ratio for Lead:Scintillator. From the proposal "The High Resolution Spaghetti Hadron Calorimeter" by P. Jenni et al. NIKHFF-H187-7 (1987).

E.M. CALORIMETER

BEAM



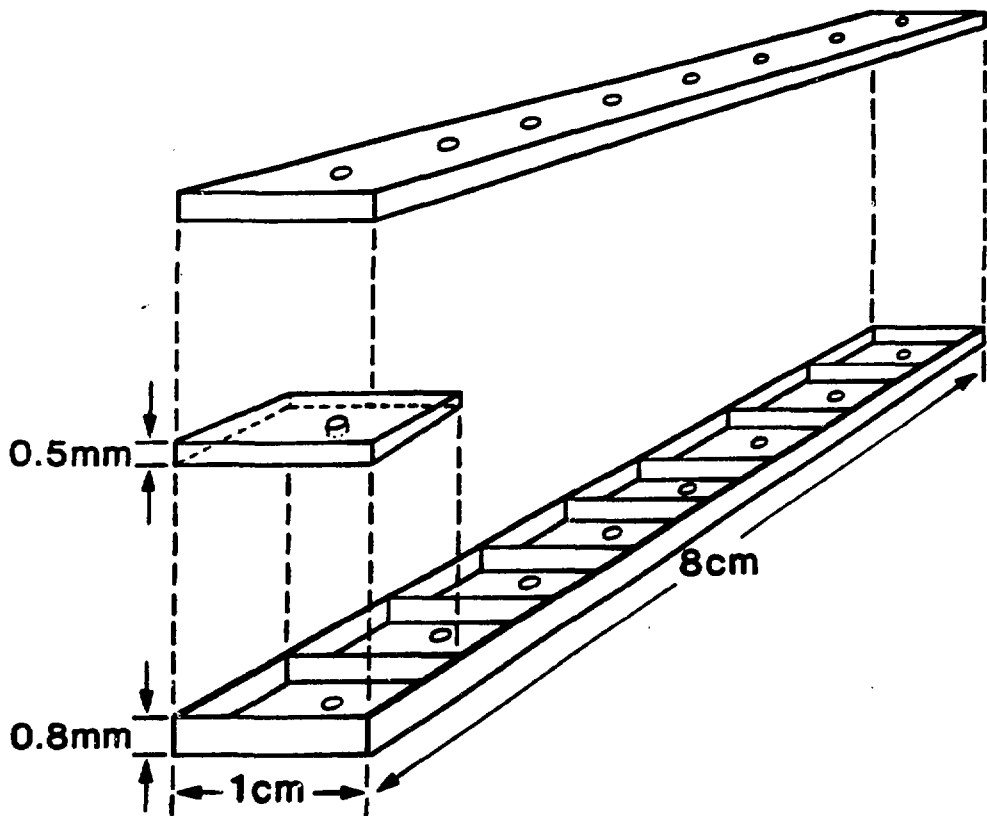
64 FIBERS
RUNNING
LENGTH OF
LEAD BLOCK



MONOLITHIC LEAD BLOCK
WITH SLOTS 1 cm X 1 mm
IN CROSS SECTION
FOR SCINTILLATOR

MECHANICAL CONSTRUCTION OF CALORIMETER

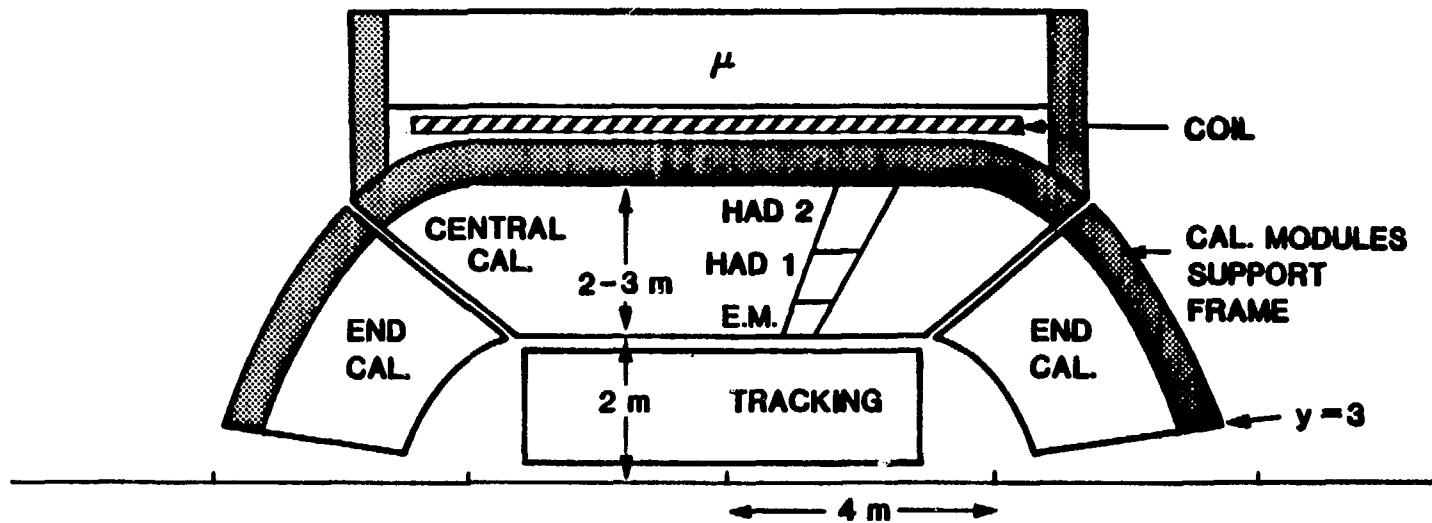
FIGURE 4 FITCAL lead block structure.



**Plastic Tray and Cover
Showing Eight Compartments
(Both Injection Molded)
With One of Eight Scintillator Tiles**

FIGURE 5 Plastic trays to be inserted in Lead Block.

FITCAL - DETECTOR LAYOUT MAGNETIC



PARAMETERS :

e.m. (40 X _o)	1.3 λ
HAD 1	3.5 λ
HAD 2	5.2 λ
	10.0 λ

WEIGHT :

CENTRAL	1438 T
END CAP x 2	2100 T
	3538 T

FIGURE 6 SSC Detector incorporating a fitcal.

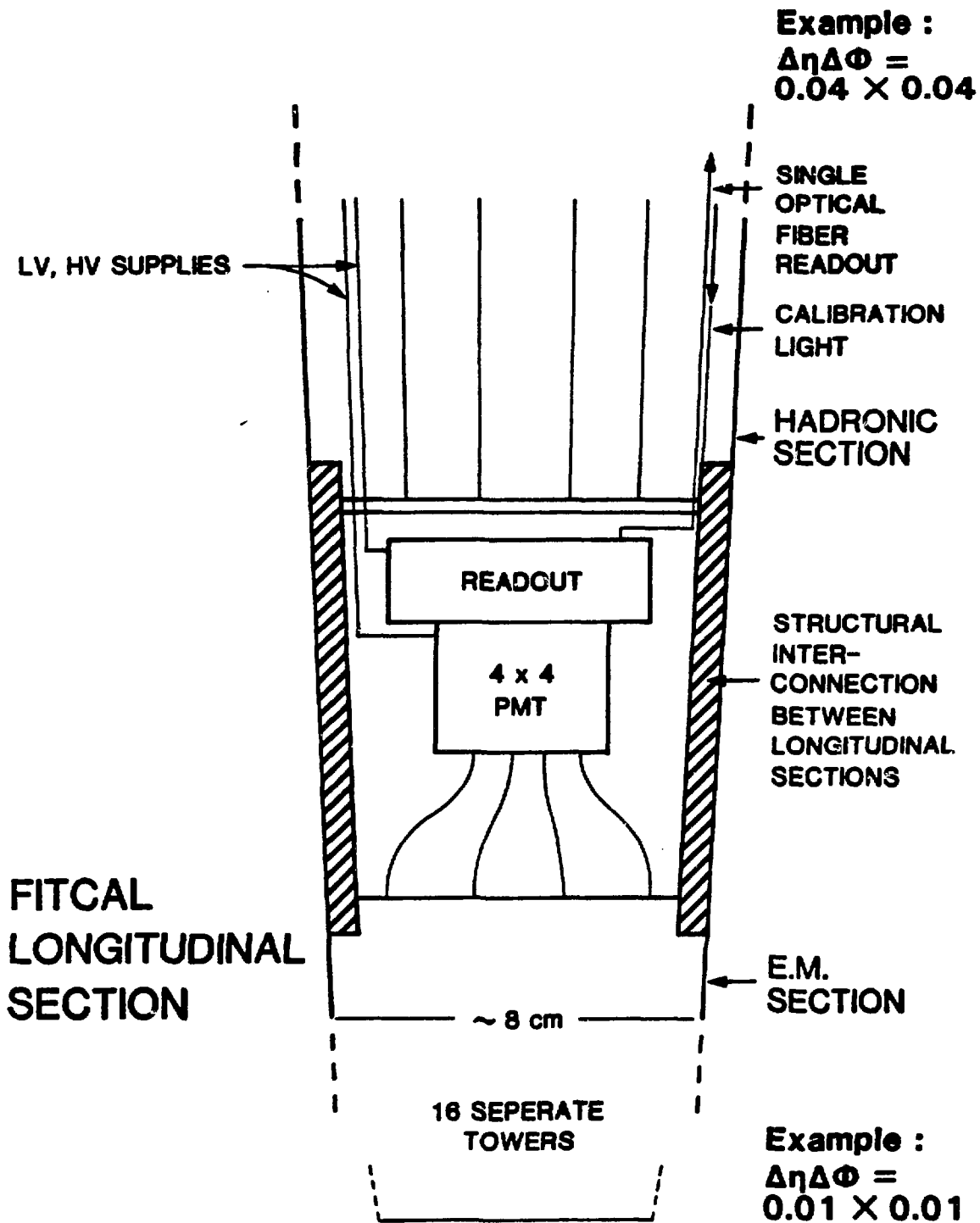


FIGURE 7 Details of readout and module interconnection for FITCAL used in FIG. (6).

FITCAL e.m. PROTOTYPE

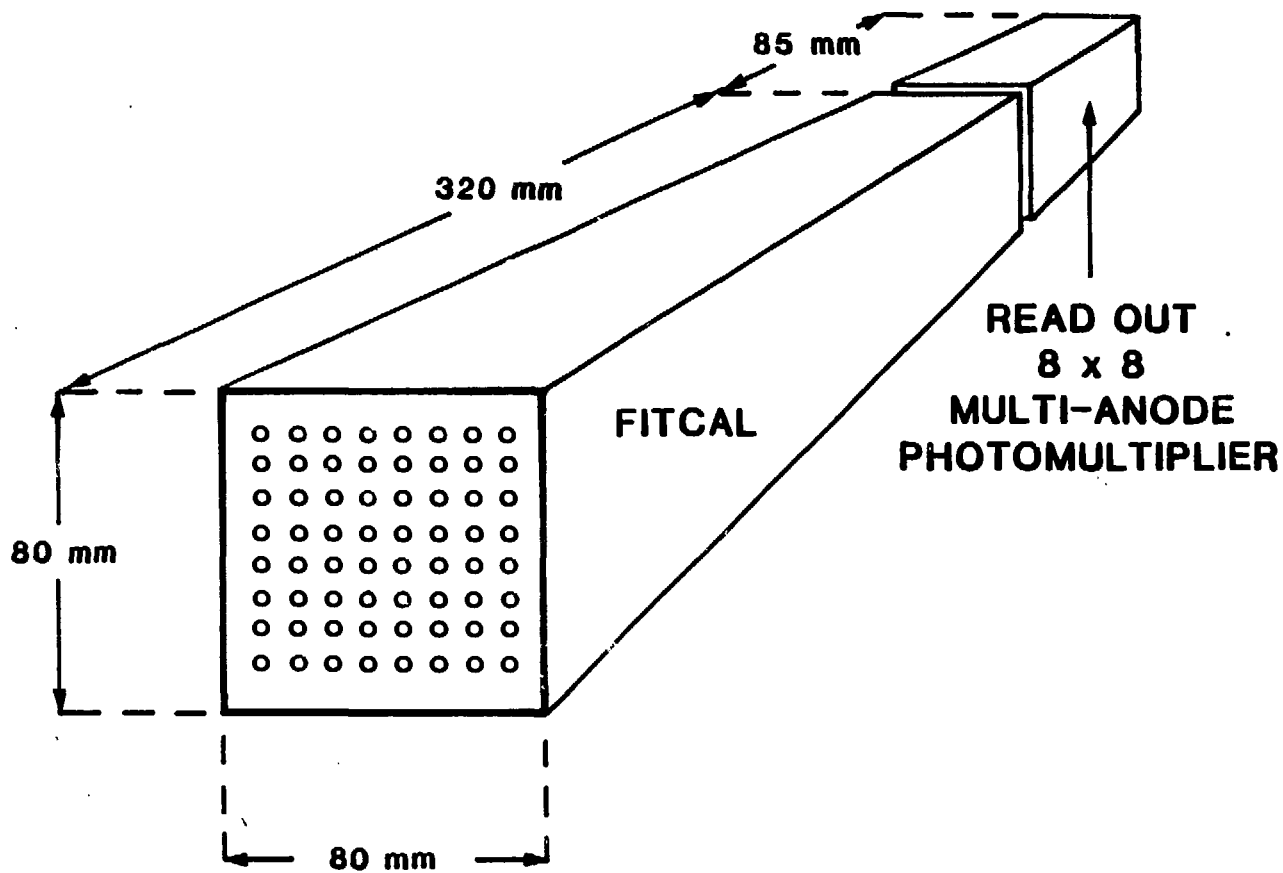


FIGURE 8 FITCAL prototype electromagnetic calorimeter module.

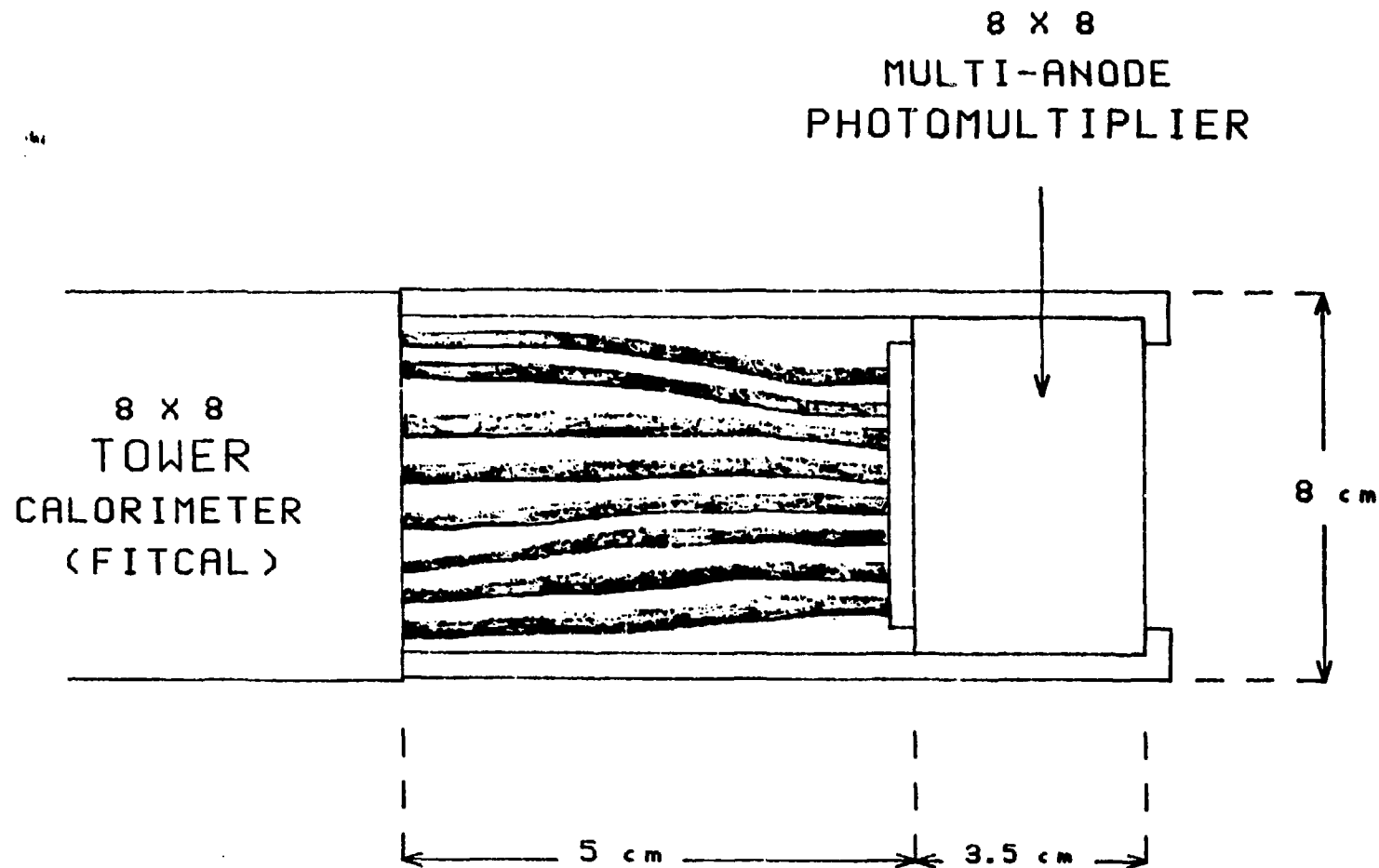


FIGURE 9 Enlarged view of readout section for module shown in FIG. (6).